Comparison of four scanning mobility particle sizers at the Fresno Supersite

John G. Watson [a,b,*], Judith C. Chow [a,b], David A. Sodeman [a,1], Douglas H. Lowenthal [a],
M.-C. Oliver Chang [a,2], Kihong Park [a,3], Xiaoliang Wang [a]

[a] Desert Research Institute, 2215 Raggio Parkway, Reno, NV, 89512, USA
[b] Institute of Earth Environment, Chinese Academy of Sciences, 10 Fenghui South Road, Xi'an High Tech Zone, Xi'an 710075, China

ABSTRACT

Size distributions of ambient aerosols at the Fresno Supersite were measured with four commercially available scanning mobility particle sizers (SMPS). TSI nano, TSI standard, Grimm, and MSP instruments were collocated at the Fresno Supersite and particle size distributions were measured continuously from August 18 through September 18, 2005. For particles with diameters between 10 and 200 nm, differences among hourly-average ambient particle concentrations ranged from 0% between the TSI nano and Grimm in the 30–50 nm size range to 39% between the Grimm and MSP in the 10–30 nm size range. MSP concentrations were 10–33% lower than those measured with the TSI standard for particles smaller than 200 nm. The TSI nano and TSI standard agreed to within 5% in their overlapping size range (10–84 nm). The TSI nano and Grimm agreed to within 40% for 5–10 nm particles.

© 2011 Chinese Society of Particuology and Institute of Process Engineering, Chinese Academy of Sciences. Published by Elsevier B.V. All rights reserved.

1. Introduction

Ultrafine (<100 nm) and fine (<2.5 μm) suspended particulate matter (PM) fractions affect human health (Chow & Watson, 2007; Mauderly & Chow, 2008; Pope & Dockery, 2006), visibility (Chow et al., 2002; Watson, 2002), and the earth's radiation balance (MacCracken, 2008; Princiotta, 2009). Because ultrafine particles contribute little to aerosol mass, $PM_{2.5}$ and PM_{10} (particles with aerodynamic diameters less than 2.5 and 10 μm, respectively) may not be appropriate indices for evaluating the effects of aerosols on human health (Biswas & Wu, 2005; Chow, Watson, Savage, et al., 2005; Seigneur, 2009).

Scanning mobility particle sizers (SMPS) are used to continuously measure the mobility size distributions of ultrafine and fine particles (Chang et al., 2004; Eleftheriadis, Nyeki, Psomiadou, & Colbeck, 2004; Lowenthal, Borys, & Wetzel, 2002; McMurry & Woo, 2002; Stolzenburg et al., 2005; Wang & Flagan, 1990; Watson et al., 2002; Watson, Chow, Park, & Lowenthal, 2006; Watson, Chow, Lowenthal, et al., 2006). The SMPS consists of a particle charge conditioner, a differential mobility analyzer (DMA), a condensation particle counter (CPC), relevant flow rate and voltage control devices, and data acquisition hardware and software (Wang & Flagan, 1990). The accuracy of the SMPS-measured size distributions depends on: (1) the DMA construction, flow rates, and voltage accuracy (Knutson & Whitby, 1975); (2) the particle charge distribution (Fuchs, 1963); (3) the CPC counting efficiency as a function of particle size (Kesten, Reineking, & Porstendorfer, 1991; Stolzenburg & McMurry, 1991); (4) particle transport time (Collins, Flagan, & Seinfeld, 2002; Russell, Flagan, & Seinfeld, 1995); and (5) particle transmission efficiency through the instrument (Reineking & Porstendörfer, 1986). The DMA transfer functions have been independently evaluated for some units (Ankilov et al., 2002a,b; Collins, Cocker, Flagan, & Seinfeld, 2004; Heim, Kasper, Reischl, & Gerhart, 2004; Stolzenburg, 1988; Wiedensohlet et al., 1997), most often using the tandem differential mobility analyzer (TDMA) with two DMAs in series (Birmili et al., 1997; Karlsson & Martinsson, 2003; Rader & McMurry, 1986; Stolzenburg, 1988). The counting efficiency of the CPC as a function of particle diameter has been evaluated with respect to electrometers and/or other CPCs using laboratory-generated monodisperse particles (Ankilov et al., 2002a,b; Collins et al., 2004; Kesten et al., 1991; Stolzenburg & McMurry, 1991; Wang, Caldow, Sem, Hama, & Sakurai, 2010; Wiedensohlet et al., 1997). Commercially available SMPS instruments use different DMAs, CPCs, flow rates, and data inversion parameters and techniques. However, the comparability of these instruments has not been very well studied, especially under real-world measurement conditions.

---

* Corresponding author at: Desert Research Institute, 2215 Raggio Parkway, Reno, NV, 89512, USA. Tel.: +1 775 674 7046; fax: +1 775 674 7009.
  E-mail address: john.watson@dri.edu (J.G. Watson).
[1] Present Address: San Diego Air Pollution Control District, San Diego, CA, USA.
[2] Present Address: California Air Resources Board, El Monte, CA, USA.
[3] Present Address: Gwangju Institute of Science and Technology, Gwangju, Korea.

Table 1
Specification of SMPS instruments used in this study.

	TSI nano	TSI standard	Grimm	MSP
Model	Model 3936N SMPS	Model 3936L SMPS	Model Grimm SMPS+C	Model 1000XP WPS
Data reduction software	Modified[a] by Mark Stolzenburg for Fresno Supersite	Modified[a] by Mark Stolzenburg for Fresno Supersite	Grimm 5.477 Version 1.33	WPS Commander Version 2.4
Number of size bins (channels)	47[c]	52[c]	44[d]	48[c]
Time per scan including down scan (s)	150[c]	150[c]	230[d]	150[c]
Inlet impactor D_{50} (nm)	~320	~420	~700	~500
Type of charge conditioner	^{85}Kr	^{85}Kr	^{210}Po	^{210}Po
DMA type	Model 3085 Nano DMA	Model 3081 Long DMA	Model 5.500 Medium M-DMA	MSP DMA
Particle size range (nm)	3–84	10–379	5–350	10–1000[b]
DMA aerosol flow rate (L/min)	1.5	1.0	0.3	0.3
DMA sheath-air flow rate (L/min)	10	7	3	3
CPC type	UCPC (Model 3025A)	CPC (Model 3010)	CPC (Model 5.403)	MSP CPC
CPC inlet flow rate/aerosol flow rate (L/min)	1.5/0.03	1.0/1.0	0.3/0.3	0.3/0.3
CPC concentration range (cm^{-3})	up to 10^5	up to 10^4	up to 10^7	up to 10^4
Nominal CPC single counting accuracy (cm^{-3})	±10% up to 10^4	±10% up to 10^4	±5% up to 2×10^5	±10% up to 10^4
Nominal CPC 50% counting size (nm)	3	10	5	4.5

[a] Software modifications were for data acquisition interfacing and did not relate to the SMPS processing algorithms.
[b] The particle size range from 10 to 300 nm was used in these comparisons.
[c] User selectable.
[d] For normal scan.

Rodrigue, Ranjan, Hopke, & Dhaniyala (2007) compared the performance of a TSI SMPS 3936-L22 (TSI Inc., Shoreview, MN, USA) and a MSP wide-range particle spectrometer (WPS XP-1000; MSP Corp., Shoreview, MN, USA) for laboratory-generated oil and carbon particles. They found that the peak diameters were comparable in the size range of 20–300 nm. The MSP WPS measured higher concentration than TSI SMPS for particles ~70 nm because the MSP WPS software corrected for size-dependent particle losses in the DMA, while the TSI did not. For particles >70 nm, the TSI SMPS concentration was 5–25% higher than the MSP WPS. Asbach et al. (2009) compared size distributions of sodium chloride and diesel soot measured by a TSI Fast Mobility Particle Sizer (FMPS), two TSI SMPS, and a Grimm SMPS (SMPS + C; Grimm AerosolTechnik GmbH & Co. KG, Ainring, Germany). The Grimm SMPS measured higher concentrations with broader distributions than the TSI SMPS.

Laboratory-generated aerosols do not represent the complex mixtures and environmental conditions (e.g., changes in temperature and relative humidity) found in ambient air. Collocated measurements by different SMPS provide more practical information on the reliability and comparability of these instruments. In this study, four SMPS instruments were collocated at the Fresno Supersite (Watson et al., 2000): (1) TSI nano SMPS (Model 3936N), which consists of a nano DMA (Model 3085) and an ultrafine CPC (UCPC; Model 3025A), hereafter referred to as the "TSI nano"; (2) TSI standard SMPS (Model 3936L), which consists of a "long" DMA (Model 3081) and a CPC (Model 3010), hereafter referred to as the "TSI standard"; (3) Grimm SMPS + C, which consists of a Vienna-type DMA (Model 5.500) and a CPC (Model 5.403), hereafter referred to as the "Grimm"; and (4) MSP WPS (Model 1000XP), which consists of a DMA, a CPC, and a laser particle spectrometer (LPS) operated in the scanning wide-range particle spectrometer (WPS) mode, hereafter referred to as the "MSP." Ambient aerosol measurements were made at the Fresno Supersite from August 18 through September 18, 2005. Inter-comparisons of particle number concentrations in discrete size intervals from the measured size distributions are presented.

2. Experimental

Ambient PM was sampled at the Fresno Supersite (3425 First Street, Fresno, CA, USA) approximately 5 km north-northeast of the downtown area. The site is located near roadways with moderate traffic and is surrounded by commercial buildings, churches, schools, and residences. Aerosols were sampled through a PM$_{2.5}$ size-selective inlet located 10 m above the ground on the rooftop of a two-story building then distributed to the four SMPS instruments located in an air-conditioned room on the second floor. The Fresno aerosol is well characterized (Chen, Watson, Chow, & Magliano, 2007; Chow et al., 1992; Chow, Watson, Lowenthal, & Magliano, 2005; Chow, Chen, et al., 2006; Chow, Watson, Lowenthal, Chen, & Magliano, 2006; Chow, Watson, Lowenthal, & Magliano, 2008; Rinehart, Fujita, Chow, Magliano, & Zielinska, 2006; Watson et al., 2002) and is composed of contributions from regional wildfires and prescribed burning, engine exhaust, secondary organic aerosol, and secondary ammonium nitrate during the study period. Ammonium sulfate contributions are small. Instrument comparability may differ from that reported here for other aerosol mixtures.

The TSI nano was operated at sample and sheath-air flow rates of 1.5 and 10 L/min, respectively, which acquired a particle size distribution (PSD) from 3 to 84 nm every 150 s. The TSI standard was operated at sample and sheath-air flow rates of 1.0 and 7 L/min, respectively, which acquired a PSD from 10–379 nm every 150 s. The Grimm was operated at sample and sheath-air flow rates of 0.3 and 3 L/min, respectively, which acquired a PSD from 5 to 350 nm every 230 s. The MSP operated at DMA sample, sheath-air, and LPS flow rates of 0.3, 3, and 0.7 L/min, respectively, and acquired a PSD from 10 nm to 10 μm every 150 s. The MSP in the 10–300 nm size range measured with the DMA and CPC were compared with those measured by the other SMPS instruments. The two TSI SMPS instruments used a ^{85}Kr charge conditioner; the Grimm and MSP used a ^{210}Po charge conditioner. All of the instruments were serviced by the manufacturers prior to the experiment. Detailed specifications of these instruments are presented in Table 1.

3. Results

Hourly average particle size distributions (dN/dlog D_p versus D_p) measured with the four SMPS instruments in Fresno Supersite are compared in Fig. 1. All PSDs are similar in shape; Fig. 1(a) shows that all instruments measured two size modes, centered at ~20 nm and at ~40 nm at 14:00 Pacific Standard Time (PST) on September 7, 2005. High concentrations at the ~20 nm peak represent photochemically-induced particle nucleation under strong
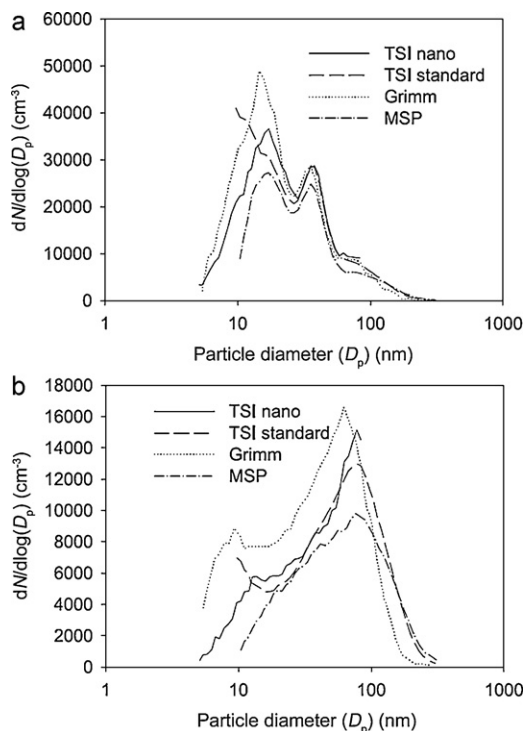
Fig. 1. Comparison of average particle size distributions measured with the TSI nano, TSI standard, Grimm, and MSP instruments at the Fresno Supersite, California for: (a) 14:00 PST on September 7, 2005; and (b) 04:00 PST on September 2, 2005.

solar radiation during summer (Watson et al., 2002). For the early morning (04:00 PST) samples collected on September 2, 2005, Fig. 1(b) shows that particle number concentrations were lower and the major size mode shifted to about 90 nm. This case probably represents a more aged aerosol. The Grimm measured higher concentrations below 100 nm but lower concentrations above 100 nm relative to the TSI standard and the MSP, which measured the lowest concentrations up to about 100 nm. The upturn at the lower end of the TSI standard PSD in Fig. 1 was attributed by Watson, Chow, Park, & Lowenthal (2006) to "time smearing" in the TSI Model 3010 CPC which occurs when the CPC counts residual particles from the previous down scan.

Studies of particle nucleation and evolution focus on the lower end of the ultrafine particle size range (i.e., <30 nm). Fig. 2 shows that hourly-average 10–30 nm particle concentrations from the different instruments were highly correlated ($0.97 \leq r \leq 1.00$) although the slopes and intercepts show differences in the absolute values. The regression slopes with respect to the TSI nano were 0.92 for the TSI standard, 1.09 for the Grimm, and 0.73 for the MSP, while intercepts varied from -7.4 cm^{-3} for the MSP to 365 cm^{-3} for the Grimm compared with the TSI nano. The TSI standard and the TSI nano provided the most comparable results in the overlap region. Average hourly particle concentrations in six size intervals (i.e., 5–10, 10–30, 30–50, 50–100, 100–200, and 200–300 nm) over the ambient sampling period are shown for each SMPS in Fig. 3. Since the reporting size intervals differ among the instruments, size distributions are expressed in concentrations per unit size (dN/dD_p) in units of (cm^{-3} nm^{-1}). The TSI nano is not included in the 50–100 nm size range in Fig. 3 because its upper size limit is 84 nm. Particles were most abundant in the 10–30 nm range, but the best agreement among the different instruments was found for the 30–50 and 100–200 nm size ranges.
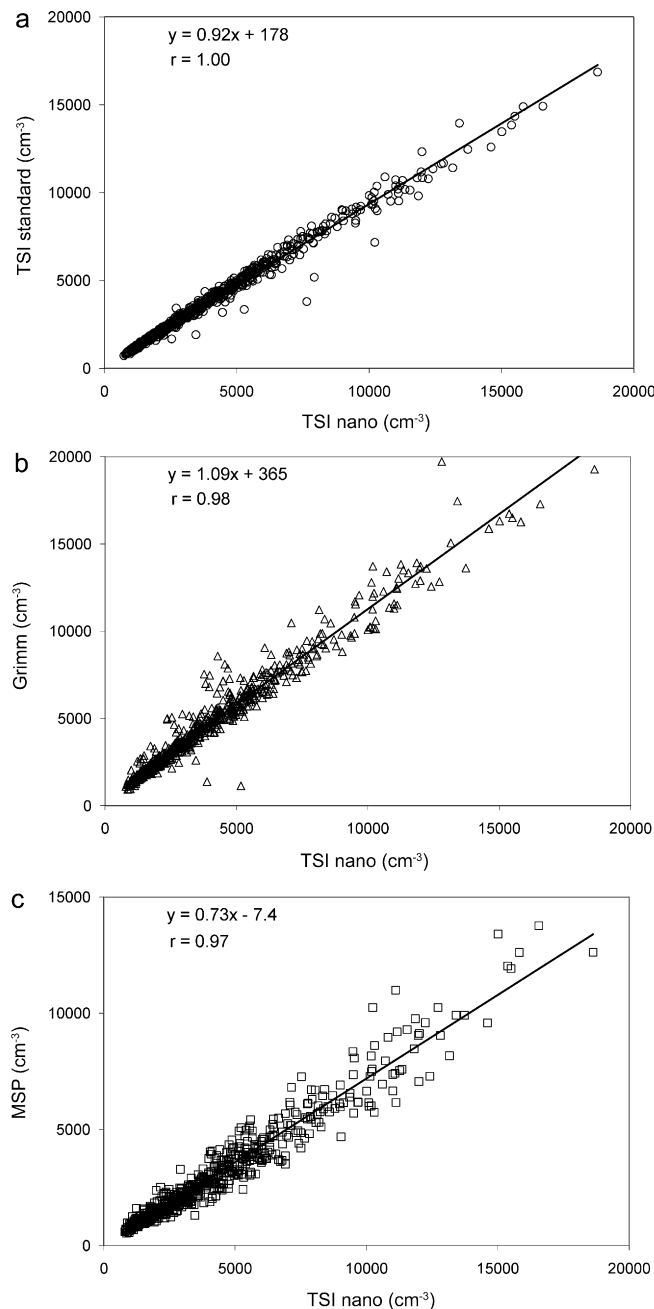

Fig. 2. Comparisons of hourly average particle concentrations (cm^{-3}) in the 10–30 nm size range [N (10–30 nm)] for the four SMPS instruments. Regression parameters are shown for: (a) TSI standard versus TSI nano; (b) Grimm versus TSI nano; and (c) MSP versus TSI nano at the Fresno Supersite between August 18, 2005 and September 18, 2005.

Table 2 compares hourly average particle concentrations per unit size for the same six size intervals. The average paired differences are defined for instruments x and y as:

$$\text{Average Difference} = \frac{100}{N} \sum \frac{y - x}{x}. \tag{1}$$

The overall average correlation is 0.92, or 0.95 for the first five size intervals (i.e., 5–200 nm). The lowest correlations of 0.55–0.74 are found for the 200–300 nm size range, among the four SMPS instruments. The largest differences of -42% to $+262\%$ also occur in the 200–300 nm size range, probably due to low concentrations in this region. The two TSI instruments agreed to within 4.8%
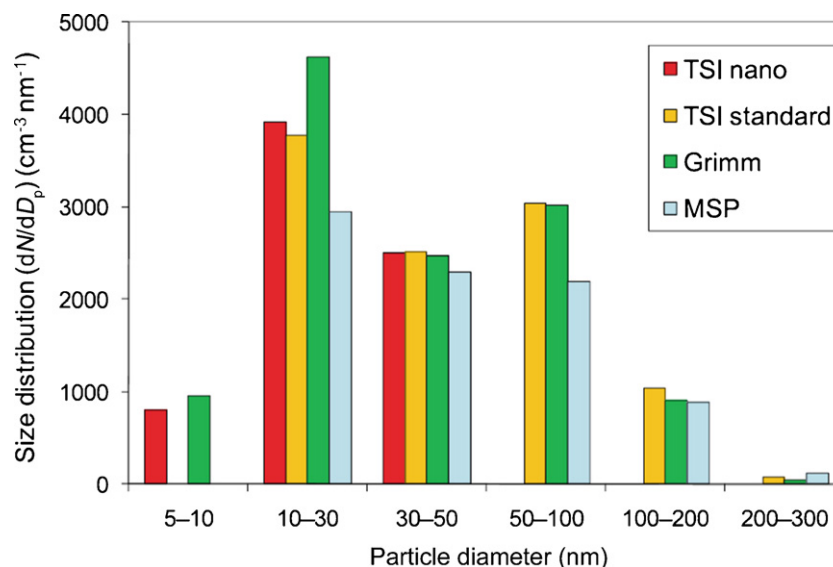
Fig. 3. Hourly average particle concentrations per unit size (cm^{-3} nm^{-1}) in six size intervals for the four SMPS instruments at the Fresno Supersite between August 18, 2005 and September 18, 2005.

for the 10–84 nm size range. The Grimm measured 40% and 23% higher concentrations than the TSI nano in the 5–10 and 10–30 nm intervals, respectively, the same concentrations (on average) in the 30–50 nm size range, and 0.1% lower concentrations in the 50–84 nm size range. The Grimm measured 16.3% lower concentrations than the TSI standard in the 100–200 nm size range. The MSP yielded 10–33% lower concentrations compared to the two TSI instruments for D_p < 200 nm, and reported 39% lower concentrations than the Grimm for the 10–30 nm size range.

The statistical moments of the PSD have been used to describe aerosol optical, growth, and cloud activation properties (McGraw, Nemesure, & Schwartz, 1998; Wright et al., 2002). It is thus useful to compare the particle sizes measured with the different SMPS instruments in terms of their central tendencies and variances, which are represented by the geometric mean diameter (D_g) and standard deviation (S_g). For the 10–300 nm range, the time series plot in Fig. 4 shows that 24-h average D_g and S_g for the TSI standard, Grimm, and MSP measurements were 41 ± 2.0, 37 ± 1.9, and

Table 2
Comparisons of hourly-average particle concentrations per unit size (cm^{-3} nm^{-1}) in six size intervals measured with four SMPS instruments at the Fresno Supersite.

Size range	SMPS instrument		Avg. of y	Avg. of x	Number of pairs	Average difference	Correlation (r)	Regression slope	Regression intercept
	y	x	(cm^{-3} nm^{-1})			(%)[a]			(cm^{-3} nm^{-1})
N (5–10 nm)	Grimm	TSI nano	210	161	704	40	0.91	1.18	19.7
N (10–30 nm)	TSI standard	TSI nano	188	196	764	−2.1	0.99	0.92	8.9
	Grimm	TSI nano	232	195	704	23	0.98	1.09	18.3
	MSP	TSI nano	147	203	681	−27	0.97	0.73	−0.4
	Grimm	TSI standard	232	188	704	26	0.97	1.18	9.8
	MSP	TSI standard	147	195	681	−25	0.96	0.78	−4.9
	MSP	Grimm	147	240	629	−39	0.96	0.64	−7.5
N (30–50 nm)	TSI standard	TSI nano	126	125	764	1.2	0.99	0.96	5.4
	Grimm	TSI nano	123	127	704	0.0	0.94	0.84	17.0
	MSP	TSI nano	115	127	681	−9.6	0.98	0.89	1.50
	Grimm	TSI standard	123	127	704	−1.2	0.95	0.88	11.7
	MSP	TSI standard	115	127	681	−10.5	0.98	0.92	−2.9
	MSP	Grimm	116	125	629	−6.8	0.95	0.96	−4.3
N (50–100 nm)	TSI standard	TSI nano[b]	76	79	764	−4.8	0.99	0.97	−1.10
	Grimm	TSI nano[b]	80	80	704	−0.1	0.93	0.97	2.2
	MSP	TSI nano[b]	53	78	681	−33	0.98	0.68	−0.80
	Grimm	TSI standard	60	61	704	−1.4	0.93	0.97	1.00
	MSP	TSI standard	44	60	681	−27	0.98	0.72	0.50
	MSP	Grimm	44	60	629	−24	0.92	0.65	5.3
N (100–200 nm)	Grimm	TSI standard	9	10	704	−16.3	0.87	0.89	−0.30
	MSP	TSI standard	9	10	681	−13.0	0.99	0.86	0.10
	MSP	Grimm	9	9	629	19.5	0.86	0.72	2.5
N (200–300 nm)	Grimm	TSI standard	0.4	0.7	704	−42	0.74	0.45	0.10
	MSP	TSI standard	1.1	0.7	681	62	0.73	1.48	0.10
	MSP	Grimm	1.1	0.4	629	262	0.55	1.76	0.40

[a] Average difference = $\frac{100}{N} \sum \frac{y-x}{x}$.
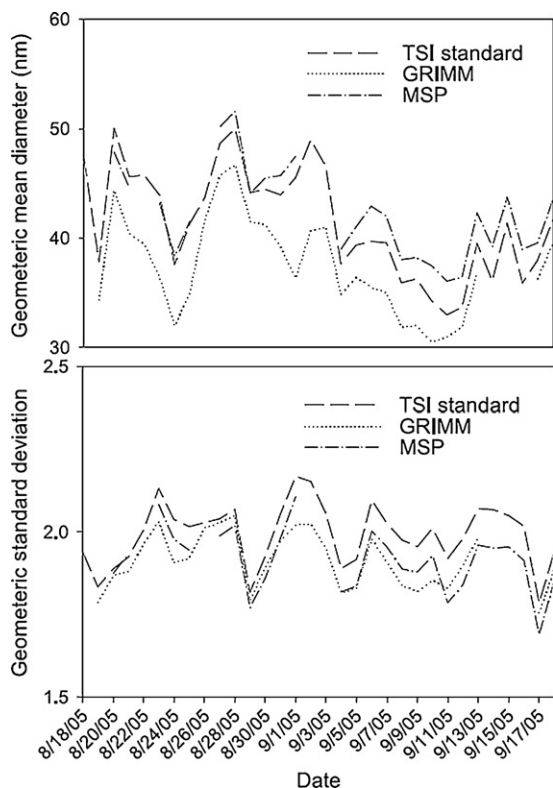[b] N (50–84 nm) was used for comparisons with the TSI nano SMPS.

Fig. 4. Time series of 24-h average geometric mean diameter (D_g) and geometric standard deviation (S_g) for the 10–300 nm range measured with the TSI standard, Grimm, and MSP instruments at the Fresno Supersite between August 18, 2005 and September 18, 2005.

42 ± 1.9 nm, respectively. The ~5% lower D_g for the Grimm is consistent with its relatively higher concentrations in the smaller size intervals (Table 2). The S_g averages were the same within $\pm 5\%$. These parameters were well correlated ($r > 0.92$ for D_g and $r > 0.89$ for S_g) among different SMPS instruments. Malm and Pitchford (1997) reported inverse relationships between D_g and S_g at sites in the Grand Canyon. However, correlations between 24-h average D_g and S_g in Fresno were only 0.22, 0.46, and 0.45 for the TSI standard, Grimm, and MSP size distributions, respectively. This may be due to Malm and Pitchford (1997) having reported particle mass while this study is based on particle number.

4. Summary and conclusions

TSI nano, TSI standard, Grimm SMPS + C, and MSP WPS instruments were compared at the Fresno Supersite from August 18 through September 18, 2005. Similarly shaped particle size distributions were found among the four instruments. For particles between 10 and 200 nm, the difference between instruments ranged from 0% between the TSI nano and Grimm in the 30–50 nm size range to 39% between the Grimm and MSP in the 10–30 nm size range for hourly average concentrations. Larger discrepancies (40–262%) were found for small (5–10 nm) and large (200–300 nm) particle size ranges. The TSI nano and TSI standard SMPS agreed to within 1–5% in the 10–84 nm size range. MSP concentrations were consistently 10–33% lower than those measured by the two TSI instruments for $D_p < 200$ nm.

Differences among SMPS instruments may be related to differences in particle charging efficiency, CPC counting efficiency, diffusion losses, and non-ideal DMA transfer functions. The charging efficiency as a function of particle size was theoretically

determined from Fuchs (1963) theory for each SMPS, providing almost the same efficiency curve among instruments. However, the actual efficiencies of the charge conditioners are unknown and could have been different. Similarly, theoretical DMA transfer functions are used in the data reduction software. But the actual DMA transfer functions might deviate from the ideal model due to imperfect machining, for example. Each manufacturer determines a universal CPC counting efficiency curve to correct concentration data in each SMPS instrument. Such counting efficiency curves are generally determined on a single CPC, and not every CPC sold is individually calibrated. Most SMPS instrument end-users do not have the resources required to rigorously evaluate their performance. The results presented in this study represent the order of measurement uncertainty that users can expect in real-world applications to an urban aerosol. Rigorous experiments and better documentation of the assumptions inherent in the data processing software for each instrument are needed to determine the actual causes of the differences.

Acknowledgments

References

Ankilov, A., Colhoun, M., Enderle, K.-H., Gras, J., Julanov, Y., Kaller, D., et al. (2002a). Intercomparison of number concentration measurements by various aerosol particle counters. *Atmospheric Research*, *62*, 177–207.

Ankilov, A., Colhoun, M., Enderle, K.-H., Gras, J., Julanov, Y., Kaller, D., et al. (2002b). Particle size dependent response of aerosol counters. *Atmospheric Research*, *62*, 209–237.

Asbach, C., Kaminski, H., Fissan, H., Monz, C., Dahmann, D., Mulhopt, S., et al. (2009). Comparison of four mobility particle sizers with different time resolution for stationary exposure measurements. *Journal of Nanoparticle Research*, *11*, 1593–1609.

Birmili, W., Stratmann, F., Wiedensohler, A., Covert, D., Russell, L. M., & Berg, O. (1997). Determination of differential mobility analyzer transfer functions using identical instruments in series. *Aerosol Science and Technology*, *27*, 215–223.

Biswas, P., & Wu, C. Y. (2005). 2005 Critical review: Nanoparticles and the environment. *Journal of the Air & Waste Management Association*, *55*, 708–746.

Chang, M.-C. O., Chow, J. C., Watson, J. G., Hopke, P. K., Yi, S. M., & England, G. C. (2004). Measurement of ultrafine particle size distributions from coal-, oil-, and gas-fired stationary combustion sources. *Journal of the Air & Waste Management Association*, *54*, 1494–1505.

Chen, L.-W. A., Watson, J. G., Chow, J. C., & Magliano, K. L. (2007). Quantifying PM₂.₅ source contributions for the San Joaquin Valley with multivariate receptor models. *Environmental Science & Technology*, *41*(8), 2818–2826.

Chow, J. C., & Watson, J. G. (2007). Survey of measurement and composition of ultrafine particles. *Aerosol and Air Quality Research*, *7*, 121–173.

Chow, J. C., Bachmann, J. D., Wierman, S. S. G., Mathai, C. V., Malm, W. C., White, W. H., et al. (2002). 2002 Critical review discussion—Visibility: Science and regulation. *Journal of the Air & Waste Management Association*, *52*, 973–999.

Chow, J. C., Chen, L.-W. A., Watson, J. G., Lowenthal, D. H., Magliano, K. L., Turkiewicz, K., et al. (2006). PM₂.₅ chemical composition and spatiotemporal variability during the California Regional PM₁₀/PM₂.₅ Air Quality Study (CRPAQS). *Journal of Geophysical Research: Atmospheres*, *111*(D10S04), 1–17. doi:10.1029/2005JD006457

Chow, J. C., Watson, J. G., Lowenthal, D. H., Chen, L.-W. A., & Magliano, K. L. (2006). Particulate carbon measurements in California's San Joaquin valley. *Chemosphere*, *62*(3), 337–348.

Chow, J. C., Watson, J. G., Lowenthal, D. H., & Magliano, K. L. (2005). Loss of PM₂.₅ nitrate from filter samples in central California. *Journal of the Air & Waste Management Association*, *55*(8), 1158–1168.

Chow, J. C., Watson, J. G., Lowenthal, D. H., & Magliano, K. L. (2008). Size-resolved aerosol chemical concentrations at rural and urban sites in Central California, USA. *Atmospheric Research*, *90*, 243–252. doi:10.1016/j.atmosres.2008.03.017

Chow, J. C., Watson, J. G., Lowenthal, D. H., Solomon, P. A., Magliano, K. L., Ziman, S. D., et al. (1992). PM₁₀ source apportionment in California's San Joaquin Valley. *Atmospheric Environment*, *26A*(18), 3335–3354.

Chow, J. C., Watson, J. G., Savage, N., Solomon, J., Cheng, Y. S., McMurry, P. H., et al. (2005). 2005 Critical review discussion: Nanoparticles and the environment. *Journal of the Air & Waste Management Association, 55*, 1411–1417.

Collins, D. R., Cocker, D. R., Flagan, R. C., & Seinfeld, J. H. (2004). The scanning DMA transfer function. *Aerosol Science and Technology, 38*, 833–850.

Collins, D. R., Flagan, R. C., & Seinfeld, J. H. (2002). Improved inversion of scanning DMA data. *Aerosol Science and Technology, 36*, 1–9.

Eleftheriadis, K., Nyeki, S., Psomiadou, C., & Colbeck, I. (2004). Background aerosol properties in the European arctic. *Water Air and Soil Pollution, 4*, 23–30.

Fuchs, N. A. (1963). On the stationary charge distribution on aerosol particles in a bipolar ionic atmosphere. *Geofisica Pura e Applicata, 56*, 185–193.

Heim, M., Kasper, G., Reischl, G. P., & Gerhart, C. (2004). Performance of a new commercial electrical mobility spectrometer. *Aerosol Science and Technology, 38*, 3–14.

Karlsson, M. N. A., & Martinsson, B. G. (2003). Methods to measure and predict the transfer function size dependence of individual DMAS. *Journal of Aerosol Science, 34*, 603–625.

Kesten, J., Reineking, A., & Porstendorfer, I. (1991). Calibration of a TSI Model 3025 ultrafine condensation particle counter. *Aerosol Science and Technology, 15*, 107–111.

Knutson, E. O., & Whitby, K. T. (1975). Aerosol classification by electric mobility: Apparatus, theory, and applications. *Journal of Aerosol Science, 6*, 443–451.

Lowenthal, D. H., Borys, R. D., & Wetzel, M. A. (2002). Aerosol distributions and cloud interactions at a mountaintop laboratory. *Journal of Geophysical Research, 108*, 4345–4351.

MacCracken, M. C. (2008). Critical review: Prospects for future climate change and the reasons for early action. *Journal of the Air & Waste Management Association, 58*, 735–786.

Malm, W. C., & Pitchford, M. L. (1997). Comparison of calculated sulfate scattering efficiencies as estimated from size-resolved particle measurements at three national locations. *Atmospheric Environment, 31*, 1315–1325.

Mauderly, J. L., & Chow, J. C. (2008). Health effects of organic aerosols. *Inhalation Toxicology, 20*, 257–288.

McGraw, R., Nemesure, S., & Schwartz, S. E. (1998). Properties and evolution of aerosols with size distributions having identical moments. *Journal of Aerosol Science, 29*, 761–772.

McMurry, P. H., & Woo, K. S. (2002). Size distributions of 3–100 nm urban Atlanta aerosols: Measurement and observations. *Journal of Aerosol Medicine, 15*, 169–178.

Pope, C. A., III, & Dockery, D. W. (2006). Critical review: Health effects of fine particulate air pollution: Lines that connect. *Journal of the Air & Waste Management Association, 56*, 709–742.

Princiotta, F. (2009). Global climate change and the mitigation challenge. *Journal of the Air & Waste Management Association, 59*, 1194–1211.

Rader, D. J., & McMurry, P. H. (1986). Application of the tandem differential mobility analyzer to studies of droplet growth or evaporation. *Journal of Aerosol Science, 17*, 771–787.

Reineking, A., & Porstendörfer, J. (1986). Measurements of particle loss functions in a differential mobility analyzer (TSI, Model 3071) for different flow rates. *Aerosol Science and Technology, 5*, 483–486.

Rinehart, L. R., Fujita, E. M., Chow, J. C., Magliano, K. L., & Zielinska, B. (2006). Spatial distribution of PM$_{2.5}$ associated organic compounds in central California. *Atmospheric Environment, 40*(2), 290–303.

Rodrigue, J., Ranjan, M., Hopke, P. K., & Dhaniyala, S. (2007). Performance comparison of scanning electrical mobility spectrometers. *Aerosol Science and Technology, 41*, 360–368.

Russell, L. M., Flagan, R. C., & Seinfeld, J. H. (1995). Asymmetric instrument response resulting from mixing effects in accelerated DMA-CPC measurements. *Aerosol Science and Technology, 23*, 491–509.

Seigneur, C. (2009). Current understanding of ultrafine particulate matter emitted from mobile sources. *Journal of the Air & Waste Management Association, 59*, 3–17.

Stolzenburg, M.R., (1988). An ultrafine aerosol size distribution measuring system. *Unpublished doctoral dissertation*. University of Minnesota.

Stolzenburg, M. R., & McMurry, P. H. (1991). An ultrafine aerosol condensation nucleus counter. *Aerosol Science and Technology, 14*, 48–65.

Stolzenburg, M. R., McMurry, P. H., Sakurai, H., Smith, J. N., Mauldin, R. L., Eisele, F. L., et al. (2005). Growth rates of freshly nucleated atmospheric particles in Atlanta. *Journal of Geophysical Research: Atmospheres, 110*, D22S05.

Wang, S. C., & Flagan, R. C. (1990). Scanning electrical mobility spectrometer. *Aerosol Science and Technology, 13*, 230–240.

Wang, X. L., Caldow, R., Sem, G. J., Hama, N., & Sakurai, H. (2010). Evaluation of a condensation particle counter for vehicle emission measurement: Experimental procedure and effects of calibration aerosol material. *Journal of Aerosol Science, 41*, 306–318.

Watson, J. G. (2002). Visibility: Science and regulation. *Journal of the Air & Waste Management Association, 52*, 628–713.

Watson, J. G., Chow, J. C., Bowen, J. L., Lowenthal, D. H., Hering, S. V., Ouchida, P., et al. (2000). Air quality measurements from the Fresno Supersite. *Journal of the Air & Waste Management Association, 50*, 1321–1334.

Watson, J. G., Chow, J. C., Lowenthal, D. H., Stolzenburg, M. R., Kreisberg, N. M., & Hering, S. V. (2002). Particle size relationships at the Fresno Supersite. *Journal of the Air & Waste Management Association, 52*, 822–827.

Watson, J. G., Chow, J. C., Lowenthal, D. H., Kreisberg, N., Hering, S. V., & Stolzenburg, M. R. (2006). Variations of nanoparticle concentrations at the Fresno Supersite. *Science of the Total Environment, 358*, 178–187.

Watson, J. G., Chow, J. C., Park, K., & Lowenthal, D. H. (2006). Nanoparticle and ultrafine particle events at the Fresno Supersite. *Journal of the Air & Waste Management Association, 56*, 417–430.

Wiedensohlet, A., Orsini, D., Covert, D. S., Coffmann, D., Cantrell, W., Havlicek, M., et al. (1997). Intercomparison study of the size-dependent counting efficiency of 26 condensation particle counters. *Aerosol Science and Technology, 27*, 224–242.

Wright, D. L., Yu, S., Kasibhatla, P. S., McGraw, R., Schwartz, S. E., Saxena, V. K., et al. (2002). Retrieval of aerosol properties from moments of the particle size distribution for kernels involving the step function: Cloud droplet activation. *Journal of Aerosol Science, 33*, 319–337.